

Bus Protection in Time-domain

Monir Hossain, Ph.D.
Relay Settings and Configurations
Entergy Services Inc.
New Orleans, LA, USA
Email: mhoss93@entergy.com

Abstract—This article introduces a time-domain power system busbar protection technique. The idea of the technique is conceived from the absolute-value integral quantities of the partial operating currents derived from the fault current contributions of the busbar terminals. The article presents analytical derivation and graphical illustrations of the simulated event analysis to validate the proposed technique. The technique is simple, setting-free, secure, and provides ultra-fast fault detection speed.

I. INTRODUCTION

Power system is a dynamically stable system. Inception of a fault initiates instability and with time it can jeopardize the stability of a part or the whole power system. Therefore, swift fault clearing is very crucial factor to save the power system from blackout. As a connection point of several elements, each busbar is a critical point of the power system and it demands even faster fault clearance. The fault clearance time is the summation of fault identification time and interruption time. Scientists and engineers are deploying various complex protection schemes and mechanisms of fault identification and interruption for different power system elements [1]. At present day, all established bus fault identification principles work based on phasor quantities of currents and voltages. All phasor-based techniques need extreme filtering of current and voltage signals and eventually take half-cycle to several cycles to identify the fault. The delayed fault clearing is not only raising the risk of system instability, it also reduces power transfer capacity of the network [2]. Moreover, complex filtering scheme increases the size and power consumption of the protective relays and consequently, elevates the cost of the protection systems by multiplying the price of relays, size of station battery, setting works, and maintenance.

Scientists and engineers are trying to hatch the time-domain protection technique to eliminate the above-mentioned limitations of the phasor-domain. Recently, scientists have introduced time-domain protection for transmission line based on traveling wave propagation and incremental quantities [3-5]. Both techniques have several limitations and cannot be applied as a stand-alone primary or backup protection for transmission line. They also cannot be applied for busbar protection because of their distance based working principles.

In this article a time-domain busbar protection technique is proposed by using the characteristics of the absolute-value integral quantities of the partial operating currents derived from the fault current contributions of the terminals connected to the busbar. Detail analytical derivation and the simulated graphical

event illustrations are presented below for the validation of the proposed technique.

II. ANALYTICAL DERIVATION

Each phase of a power system busbar can be defined as a multi-terminal differential zone, where each terminal is a branch circuit and it can be a transmission line, generator or load. In differential protection, phasor-based operating current refers the differential current of a zone as shown in Equation (1).

$$I\phi_{op} = \sum_{j=1}^n I\phi_j \quad (1)$$

In Equation (1), n is the number of terminals of the zone, ϕ presents phase (A or B or C), and $I\phi_j$ corresponds to phasor current of each terminal.

In reference [6], [7], the concept of phasor based Partial Operating Current (POC) quantities is conceived by successive addition of terminal currents as Equation (2).

$$I\phi_{op(k)} = \sum_{j=1}^k I\phi_j + I\phi_{k+1} \quad (2)$$

In Equation (2), $I\phi_{op(k)}$ represents k^{th} POC, where $k = 1, 2, \dots, (n-1)$. Note that in an n -terminal zone, there are $(n-1)$ POCs with initial condition $I\phi_{op(0)} = I\phi_1$. The final POC which is denoted by $I\phi_{op(n-1)}$, is equal to the term differential operating current $I\phi_{op}$ shown in Equation (1).

Reference [6], [7] also have shown that during internal fault condition, all the POCs of a bus differential zone satisfy a unique characteristic as described in Equation (3). During normal operation or external fault condition, at least one of the resultant POCs does not satisfy the characteristic defined in Equation (3).

$$|I\phi_{op(k)}| > \max(|I\phi_{op(k-1)}|, |I\phi_{k+1}|) \quad (3)$$

The remaining portion of this section proves that the above characteristic is also valid for the absolute-value integral quantities of the partial operating currents derived from instantaneous fault current contributions of the busbar terminals. Instantaneous terminal current ($i\phi_j(t)$) during fault condition is the super-imposed signal of pre-fault current ($i\phi_j^{pf}(t)$) and contributed fault current ($i\phi_j^f(t)$) as defined in Equation (4).

$$i\phi_j(t) = i\phi_j^{pf}(t) + i\phi_j^f(t) \quad (4)$$

The pre-fault current $i\phi_j^{pf}(t) = i\phi_j(t - T)$, where T = time period. Therefore, contributed fault current ($i\phi_j^f(t)$) can be expressed as Equation (5).

$$i\phi_j^f(t) = i\phi_j(t) - i\phi_j(t - T) \quad (5)$$

The operating current in time-domain is the summation of fault currents contributed by each terminal as shown in Equation (6).

$$i\phi_{op}(t) = \sum_{j=1}^n i\phi_j^f(t) \quad (6)$$

In the light of Equation (2), time-domain partial operating current quantities can be defined as in Equation (7).

$$i\phi_{op(k)}(t) = \sum_{j=1}^k i\phi_j^f(t) + i\phi_{k+1}^f(t) \quad (7)$$

During internal fault, contributed fault currents for all terminals are in the same direction and therefore, the statement of Equation (8) is true for all resultant POCs, given all $i\phi_j^f(t)$ are non-zero and $i\phi_{op(0)}(t) = i\phi_1^f(t)$. In real power systems, one or more terminals connected to the busbar may not contribute any fault current. In these cases, those terminals must be excluded from the calculation.

$$|i\phi_{op(k)}(t)| > \max(|i\phi_{op(k-1)}(t)|, |i\phi_{k+1}^f(t)|) \quad (8)$$

When signals maintain the relation of Equation (8) for a period of time with initial condition equal to zero, then the absolute-value time integral of those signals maintain same relation. Before busbar fault, all contributed fault currents ($i\phi_j^f(t)$) and resultant POCs are zero; therefore, Equation (9) is true for busbar internal fault.

$$\max\left(\int |i\phi_{op(k)}(t)|\Delta t, \int |i\phi_{k+1}^f(t)|\Delta t\right) > \max\left(\int |i\phi_{op(k-1)}(t)|\Delta t, \int |i\phi_{k+1}^f(t)|\Delta t\right) \quad (9)$$

For external faults or non-faulted transient events, like cold start or load change conditions, at least one terminal current must flow in opposite direction and consequently, one or more resultant POCs does not satisfy Equation (8) as well as Equation (9).

This article employs the inherent power system characteristics described in Equation (9) to detect busbar fault without any external setting input. If and only if at any time instant, all resultant POCs of a bus differential zone satisfy Equation (9) then it is an internal fault. The characteristic of Equation (9) is applicable for each phase of bus differential zone independently. In the following section, graphical illustrations show that the fault is detectable within a few micro-seconds irrespective of fault type, inception time, and fault resistance.

III. GRAPHICAL ILLUSTRATIONS

All the graphical illustrations presented below are the EMTP based simulated events of a four-terminal busbar ($n = 4$) where two transmission lines ($j=1$ & 2), one load ($j = 3$), and one generator ($j = 4$) are connected. For simplicity, only single phase (phase-A) event analysis are shown below because the discrimination condition described in Equation (9) is independently applicable for each phase of bus differential zone. The analog current data of the following events are captured at 12kHz sampling rate. The zoomed in view of the critical points of each figure are shown in the right.

A. Cold Start Event

Figure 1 shows a cold start event, where switching started at $t=0.03$ s. Before switching all terminal currents are zero. With the start of switching, load current starts to flow in all terminals as shown in Figure 1(a). The incremental currents or false fault currents created by switching are shown in Figure 1(b). These incremental currents sustain for only one cycle because after one cycle, $iA_j(t) = iA_j(t-T)$. Figure 1(c) shows the absolute value of resultant POCs and $iA_j(t)$. The absolute value integral quantities of POCs and $iA_j(t)$ are illustrated in Figure 1(d) and it clearly shows $\int |iA_{op3}(t)|\Delta t < \int |iA_4^f(t)|\Delta t$ for all time instant starting from switching point. Therefore, expectedly Equation (9) is not true for $\int |iA_{op3}(t)|\Delta t$ during cold start or load change.

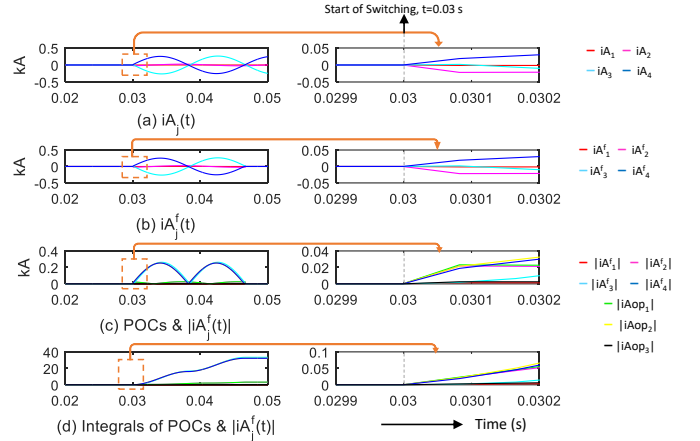


Fig. 1. Cold start event

B. Internal Fault Event I

An A-B internal fault event is illustrated in Figure 2, where fault started near zero-crossing ($t=0.050081$ s). Figure 2(a) and Figure 2(b) present instantaneous terminal currents and contributed fault currents, respectively. The fault currents remain high for only one cycle. After one cycle, fault currents become negligible because $iA_j(t) = iA_j(t-T)$. The absolute value of resultant POCs and $iA_j(t)$ are shown in Figure 2(c). Figure 2(d) presents the absolute value integral quantities of POCs and $iA_j(t)$. From the zoomed in view of Figure 2(d), it is clear that just after fault inception all resultant POCs

satisfy the condition of Equation (9) as anticipated. Therefore, the internal fault is identified in next time step ($t=0.050123s$) after fault inception. The fault detection time is only $42\mu s$.

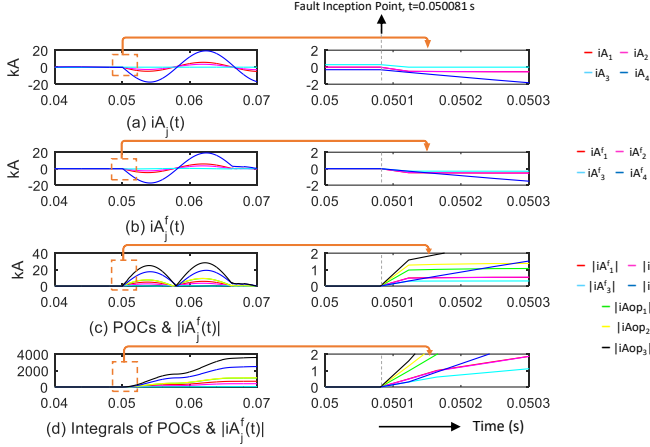


Fig. 2. A-B internal fault event

C. Internal Fault Event II

Figure 3 presents a high resistive ($R_f = 500\Omega$) A-G internal fault incepted at $t=0.050081s$ which is about 90° from zero-crossing. Figure 3(a) and Figure 3(b) display instantaneous terminal currents and contributed fault currents, respectively. The contributed fault currents are comparatively small due to high fault resistance. Figure 3(c) shows the absolute value of resultant POCs and $i_{A_j}(t)$. The absolute value integral quantities of POCs and $i_{A_j}(t)$ are illustrated in Figure 3(d). The zoomed in view of Figure 3(d) shows that all resultant POCs satisfy the condition of Equation (9) just after fault inception. The internal fault is detected as fast as in next time step ($t=0.050123s$). The fault detection time is only $42\mu s$ even for high resistive fault.

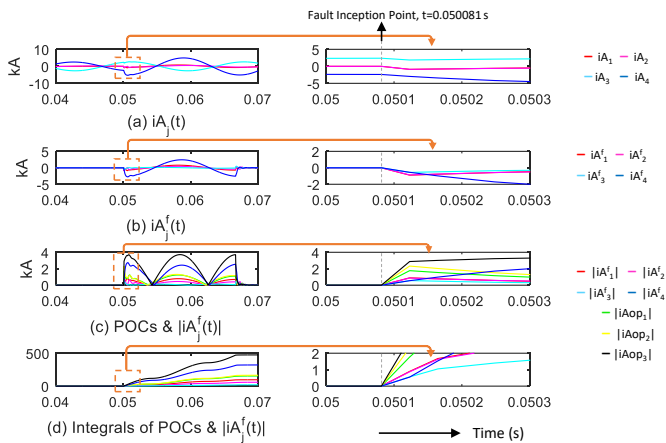


Fig. 3. A-G internal fault event

D. External Fault Event

A close-in external fault event involving phase A and ground is illustrated in Figure 4. The fault inception time $t=0.050081s$. The instantaneous terminal currents and contributed fault currents are presented in Figure 4(a) and Figure 4(b), respectively. Figure 4(c) shows the current signal of terminal 3 ($j = 3$) became distorted due to current transformer (CT) saturation. The absolute value of resultant POCs and $i_{A_j}(t)$ are shown in Figure 4(c). Figure 4(d) presents the absolute value integral quantities of POCs and $i_{A_j}(t)$ and it clearly shows $\int |i_{Aop_3}(t)|\Delta t < \int |i_{A_4^f}(t)|\Delta t$ for all time instant starting from fault inception. Therefore, Equation (9) is not true for $\int |i_{Aop_3}(t)|\Delta t$ and the proposed technique correctly detects external fault even with presence of CT saturation.

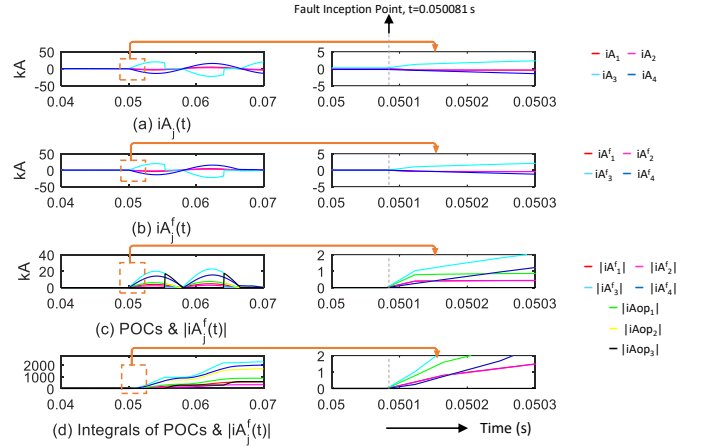


Fig. 4. A-G external fault event

IV. CONCLUSION

Both analytical derivation and graphical event illustrations validate the effectiveness of the proposed time-domain busbar protection technique. Graphical illustrations show that in time-domain the internal fault is detectable within few microseconds from the inception instant, irrespective of the fault inception time, fault types, and fault resistance. The proposed technique is also highly secured for any load change and external fault events. Mathematical formulation proves the proposed technique does not require any external setting input and it uses raw current signal data in all calculations without filtering. In summary, the article opens the door for a new bus protection domain which is simple and offers ultra-fast fault detection without sacrificing system security.

REFERENCES

- [1] F. A. M. Vasques, K. M. Silva, "Instantaneous-power-based busbar numerical differential protection", IEEE Trans. Power Deliv., vol. 34, no. 2, pp. 616-626, 2019.
- [2] R. B. Eastvedt, "The need for ultra-fast fault clearing", the proceedings of the 3rd Annual Western Protective Relay Conference, Spokane, WA, 1976.
- [3] P. Jafarian, M. Sanaye-Pasand, "A traveling-wave-based protection technique using wavelet/PCA analysis", IEEE Trans. Power Deliv., vol. 25, no. 2, pp. 588-599, 2010.

- [4] X. Dong, S. Luo, S. Shi, B. Wang, S. Wang, L. Ren, F. Xu, "Implementation and application of practical traveling-wave-based directional protection in UHV transmission lines", *IEEE Trans. Power Deliv.*, vol. 31, no. 1, pp. 294-302, 2016.
- [5] E. O. Schweitzer, B. Kaszenny, M. Mynam, A. Guzman, V. Skendzic, "New time-domain line protection principles and implementation", 8th Annual Protection, Automation and Control World Conference, Wroclaw, Poland, 2017.
- [6] M. Hossain, I. Leevongwat, P. Rastgoufard, "Partial operating current characteristics to discriminate internal and external faults of differential protection zone during CT saturation", *IET Generation, Transmission & Distribution*, vol. 12, no. 2, pp. 379-387, 2018.
- [7] M. Hossain, I. Leevongwat and P. Rastgoufard, "Design and testing of a bus differential protection scheme using partial operating current (POC) algorithm," *Elsevier Electric Power Systems Research*, vol. 157, pp. 29-38, 2018.